

CFD Hydrodynamics Analysis of Syngas Flow in Slurry Bubble Column

Artur Wodolański^{1,*}

¹ Central Mining Institute, Plac Gwarkow 1, 40-166 Katowice, Poland

ARTICLE INFO

Article history:

Received: April 28, 2016

Accepted: November 21, 2016

Keywords:

Hydrodynamics

Slurry bubble column

CFD modelling

* Corresponding author;

E-mail:

awodolazski@gig.katowice.pl

Tel.: +48 32 3246528

Fax: +48 32 3246528

ABSTRACT

In this paper, a CFD model of syngas flow in slurry bubble column was developed. The model is based on an Eulerian-Eulerian approach and includes three phases: slurry of solid particles suspended in paraffin oil and syngas bubbles. Numerical calculations carried out for catalyst particles, bubble coalescence and breakup included bubble-fluid drag force and interfacial area effects. Also, the effects of solid particles existing in liquid phase were described.

1. Introduction

Bubble column reactors next to stirred tank are used to perform the mechanical fermentation processes, biological wastewater treatment plants [1], flue gas desulfurization, oxidation/hydrogenation reactions [2] and Fischer Tropsch or methanol synthesis [3,4].

The main advantages of the use of slurry bubble column are lack of any moving parts (e.g. mixers, move of agitator shaft) which significantly reduce the device power consumption. Other advantages include simple operation of the reactor, possibility of obtaining a high slurry phase concentration where the reactions takes place, excellent heat and mass transfer through the surface at low interfacial energy demand, possibility to achieve a high degree of syngas conversion and easy temperature control by providing isothermal reaction medium [5]. The main disadvantages include limitations associated with the low suspension viscosity, limited possibility to oxygen supply and the uncontrolled coalescence of the gas-liquid system. The bubble column is the possible occurrence of back-mixing in the continuous and the dispersed phase, also difficulty in separating solid particles from the suspension and scaling-up process [6,7].

The literature includes several studies about the syngas hydrodynamics features of the flow in slurry bubble column. These can be found in articles [6-10]. CFD method is a promising tool to predict the fluid dynamics of heat and mass transfer in multiphase flows. It allows the efficient design of new processes, optimization of the existing processes or shortened development cycle. CFD methods applied to descriptions of multi-bubble systems are based on the Euler-Euler and Euler-Lagrange approach. The Eulerian multi-fluid model is widely used for the flow simulations in bubble columns [11-12]. Numerical simulations of slurry allow predicting the concentration profiles, which are difficult to locate by experiments [13].

The process of bubble formation has been studied by a number of researchers [11,12,14]. Modelling of bubble size distribution in the CFD multidimensional slurry column was used by the population balance (PB) method [15]. Also, axial dispersion models were used to describe the hydrodynamics between liquid and gas phase [2,16]. In literature, CFD methods were used to describe bubble column reactor in Fischer Tropsch synthesis perceived as an alternative method of hydrocarbon generation from coal-derived syngas, also known as the indirect coal liquefaction technology [17]. The importance of using synthesis gas from coal gasification in chemical production continues to grow. Moreover, different reaction systems are working on their effective use [18]. CFD modelling methods of slurry hydrodynamics in stirrer tank reactor without baffles of different diameters of particles and bed density were described [19].

Thus, the aim of present study was to computationally study the hydrodynamics of synthesis gas bubble column flowing through the slurry catalyst. The use of solution algorithms permits accurate solving of the flow equations. The experimental section was described in Tabiś [1]. The results were used to optimize the working conditions of bubble column experimental section. Important hydrodynamics parameters as gas hold-up and solid dispersion profiles were also investigated.

2. Modelling assumptions

In this simulation, Eulerian-Eulerian approach model was adopted to describe the multiphase syngas-slurry system. These equations take the form for the transient state which they can be formulated as the mass balance equation for the phase q:

$$\frac{\partial}{\partial t}(\alpha_q q_q Y_q^j) + \nabla \cdot (\alpha_q q_q \bar{v}_q Y_q^j) = \nabla \cdot (\alpha_q q_q D_q^j \nabla Y_q^j) \quad \sum_{j=1}^J Y_q^j = 1 \quad (1)$$

Momentum equation:

$$\frac{\partial}{\partial t}(\alpha_q q_q \bar{v}_q) + \nabla \cdot (\alpha_q q_q \bar{v}_q^2) = -\alpha_q \nabla p + \nabla \cdot \bar{\tau}_q + \alpha_q \rho_q \bar{g}_q + K_{pq}(\bar{v}_p - \bar{v}_q) + \dot{m}_{pq} \bar{v}_{pq} \quad (2)$$

Continuity equation:

$$\frac{\partial}{\partial t}(\alpha_q q_q) + \nabla \cdot (\alpha_q q_q \bar{v}_q) = -\dot{m}_{qp}, \quad \sum_{q=1}^Q \alpha_q = 1 \quad (3)$$

The numerical model assumed some simplifications such that heat transfer effects were not considered and slurry was well-mixed (Stokes number of the catalyst particles is small). The evolution of bubbles size distribution was changed due to the mechanical interaction (i.e. coalescence and breakup phenomena). Therefore, the bubble size distribution can be solved by population balance model using a discrete model to prescribe where bubble size range is subdivided into several discrete bubble classes, where mass conservation equation is given by:

$$\frac{\partial(\alpha_q q_q f_i)}{\partial t} + \nabla \cdot (\alpha_q q_q \bar{v}_{gi} f_i) = S_{gi} - \dot{m}_{gs,i}, \quad \sum_{i=1}^I S_{gi} = 0, \quad \sum_{i=1}^I \dot{m}_{gs,i} = \dot{m}_{gs} \quad (4)$$

The formula describing the ratio of energy per slurry mass unit required to break the bubble is given by:

$$P(\lambda, d_i, d_j) \alpha \left(\frac{4We_{crit} \sigma_{sq}}{\rho_s d_j \bar{e}} \right) \exp \left(- \left(\frac{4We_{crit} \sigma_{sq}}{\rho_s d_j \bar{e}} \right) \right) \quad (5)$$

where bubble size distribution is given by $P(\lambda, d_i, d_j)$, and $We_{crit}=0.1$ was used for the simulation presented in this paper. The averaged turbulent eddy energy \bar{e} is given by [20]:

$$\bar{e} = 2(\varepsilon_m \lambda)^{2/3} \quad (6)$$

The interphase drag coefficient of syngas bubbles was calculated based on the expressions proposed by Ishii and Zuber (1979) [21] and given by the following equations:

$$\frac{24}{Re_{gs}} (1 + 0.1 Re_{gs}^{0.75}) = \min \left(0.666 d_{32} (g(\rho_l - \rho_g) / \sigma)^{0.5} (\alpha)^{-0.6}, \frac{8}{3} \alpha_s^2 \right) \quad (7)$$

$$\frac{24}{Re_{gs}} (1 + 0.1 Re_{gs}^{0.75}) > 0.666 d_{32} (g(\rho_l - \rho_g) / \sigma)^{0.5} (\alpha)^{-0.6}, \quad Re_{gs} = \frac{d_{32} U_{gs} \rho_s \alpha_s}{\mu_s} \quad (8)$$

These bubbles rise with basically the same velocity. Another expression can be derived by a method analogous to the one employed by Ishii and Zuber [21]. Interphase drag force is based on the Sauter diameter which, in turn, can

be obtained using the population balance model. The model of turbulence k - ε for the mixture phase was described by the equation:

$$\frac{\partial}{\partial t}(\rho_l k_l) + \nabla(\rho_l \vec{u}_l k_l) = \nabla \cdot \left(\frac{\mu_{tl}}{\text{Pr}} \nabla k_l \right) + G_l - \rho_l \varepsilon_l \quad (9)$$

$$\frac{\partial}{\partial t}(\rho_l \varepsilon_l) + \nabla(\rho_l \vec{u}_l \varepsilon_l) = -\nabla \cdot \left(\frac{\mu_{tl}}{\text{Pr}} \nabla \varepsilon_l \right) + \frac{\varepsilon_l}{k_l} (C_{d1} G_{sl} - C_{\varepsilon 2} \rho_l \varepsilon_l) \quad (10)$$

The drag coefficient was calculated as Ishii M.[21]:

$$K_{sg} = 0.125 \rho_s A_{sg}'' C_{gs}^d \left| \vec{v}_{sg} \right| \quad (11)$$

where the spherical bubble shape is the relation between interfacial area density and the bubble diameter:

$$A_{sg}'' = \frac{6 \alpha_s f_i}{d_i} \quad (12)$$

where:

$$C_{gs}^d = d_{32} \left[\sum_{i=1}^N f_i \left(\frac{d_i}{C_{gs,i}} \right)^{1/2} \right]^{-2} \quad (13)$$

Also, static pressure drop along the bed height can be expressed as:

$$\Delta P = (q_g \alpha_g + q_l \alpha_l + q_s \alpha_s) \quad (14)$$

The pressure drop in the column depends on the bed height, slurry concentration, superficial gas velocity and the operating conditions.

3. Computational mesh and CFD model

The object of the study was the own design bubble column geometry located at the bottom gas distributor. A schematic view and also dimensions of a bubble column reactor are shown in Fig. 1a) and Table 1.

Table 1. Selected reactor dimensions

Parameter	Value
Height, m	1.4
Column diameter, m	0.4
Distributor diameter, m	0.027
Distributor location from the center of the column bottom, m	0.14

Numerical grids were generated using the MixSim 2.1.10 module preparatory. Before starting simulations with the CFD reactor models, grid sensitivity tests were performed to ensure that the solutions did not obviously change by increasing the number of computational cells. The total number of computational grids for 3 cases is shown in Table 2.

Table 2. Grid resolution

Case number	Number of cells, million
Case 1	0.0219
Case 2	0.1783
Case 3	0.2989

Fig. 1b) presents the computational mesh. The grid size of 0.1783 million cells is fine enough to obtain the grid-independent results. The mesh quality was appropriate for the simulation (max angular skewness 0.81, minimum orthogonal quality of cells 0.32, maximum aspect ratio 14.81). The CFL (Courante-Friedrichse-Lewy) criterion for the numerical stability schemes was below 1 and for time step size 0.01 sec, it was 0.36.

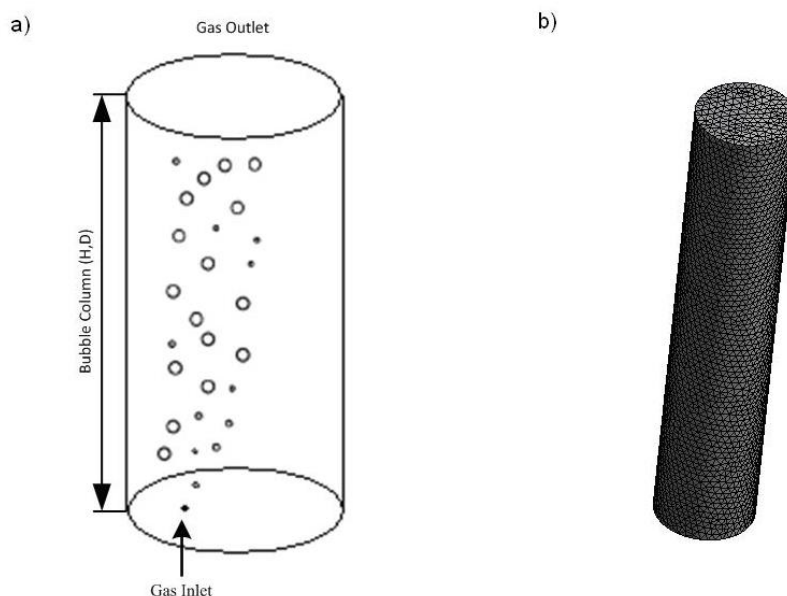


Fig.1. Schematic view of a bubble column (a), computational mesh of the bubble column used in the simulation (b)

The model was implemented into CFD code ANSYS-Fluent. The governing equations were solved using Eulerian–Eulerian model along with a standard of k - ϵ turbulence viscosity model with parameters appropriate for slurry properties to predict the adequate level of turbulent viscosity. The model derived from RANS (Reynolds averaged Navier –Stokes) was used to simulate bubble column with large numbers of bubbles [22-25]. This model was based on the transport equations for the turbulence kinetic energy (k) and its dissipation rate (ϵ). A second-order spatially accurate QUICK scheme was employed to discretize all the equations. First-order implicit time stepping was used to advance the solution in time. PISO scheme was implemented for the pressure velocity coupling. The bubble size distribution was predicted using a population balance (PB) model. Time step was chosen to be not larger than 10^{-2} and did not lead to any significant changes to time averaged values. The simulations of syngas bubble columns operated at different velocity inlets and slurry concentrations. The simulation was run for about 50 s with time step size 0.01 s. Boundary conditions and main simulation parameters are presented in Table 3.

In the present study, the effect of superficial gas velocity, initial solid concentration, gas holdup and bubble size distribution in bubble column reactor was studied. Superficial gas velocity in slurry-syngas system was a function of bubble size diameter. The catalyst particles size was about $50 \mu\text{m}$ and average solid concentration in slurry was changed to maximal value of 50 % volume fraction.

Table 3. Boundary conditions and main simulation parameters

Parameter	Value
Inlet boundary	Velocity inlet: 0.05-0.3 m/s; The gas mixture composition, % mol: 65% H ₂ , 25% CO, 5% CO ₂ , 5% N ₂
Outlet boundary	Outlet pressure: 101325;1013250 Pa
Wall boundary	Slip conditions, wall temperature: 296,15 K
Spatial Discretization	
Gradient	Green-Gauss Cell Based
Pressure	Body Force Weighted
Momentum	QUICK
Volume Fraction	QUICK
Transient formulation	First Order Implicit
Under-Relaxation Factor	
Pressure	0.5
Density	0.8
Momentum	0.4
Slip Velocity	0.1
Volumn fraction	0.8

As discussed in chapter 3, a user-defined function (UDF) was implemented for the bubble size distribution calculations. A good convergence of the calculations was obtained with a time step equal to $1 \cdot 10^{-4}$ s.

4. Results and discussion

The main goal of the present study was to numerically study the syngas hydrodynamics and bubbles population balance. In order to verify that the simulations had converged, the residuals as well as the additional parameters namely turbulence dissipation, turbulence kinetic energy and velocity were monitored. The absolute convergence criterion was specified as the residual values of 0.0001. The convergence occurs when the residuals are small enough although they may be decreasing.

The numerical study of the syngas hydrodynamics in slurry bubble column reactor was a transient simulation. Several computational runs were carried out to mainly predict the cross section volume fraction of the syngas bubbles under different time conditions. Fig. 2 shows the volume fraction profiles of the syngas bubbles under different times at 7s intervals from 1s to 22s of the bubble column cross section. Fig.3. presents the volume fraction profiles of the syngas bubbles at 7 s intervals from 29s to 43s. Increasing the syngas velocity at the inlet to the reactor also increased the gas hold-up. Moreover, approaching the gas bubbles to the interface gas hold-up increased as a result of cracking and coalescence of the syngas bubbles. The break-up of the bubbles significantly increased the concentration and the possibility of coalescence occurrence.

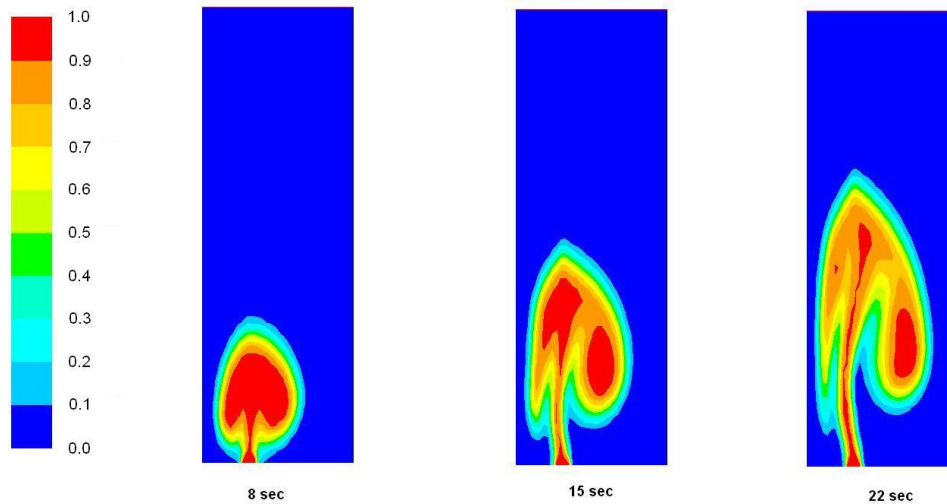


Fig. 2. Cross-section contours of syngas bubble volume fraction under different times at 7s intervals from 1s to 22s (0.1 m/s superficial gas velocity on inlet)

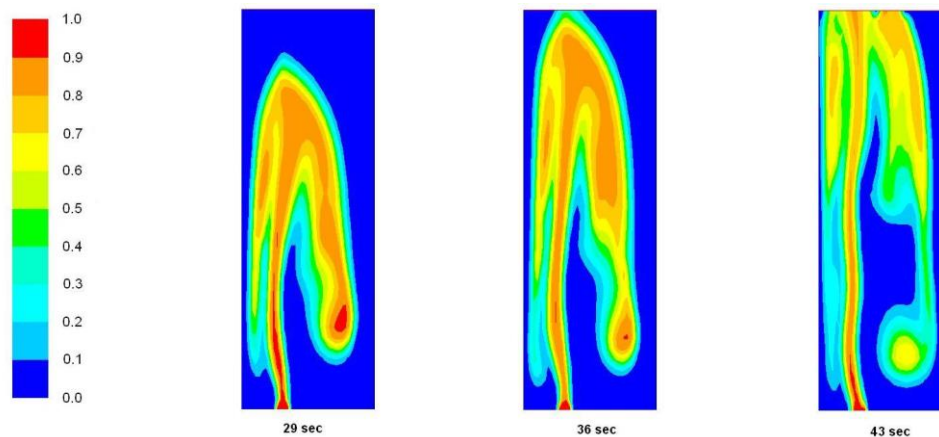


Fig. 3. Cross-section contours of syngas bubble volume fraction under different times at 7s intervals from 29s to 43s (0.1 m/s superficial gas velocity on inlet)

Fig. 4 presents streamlines of the sample syngas velocity at the inlet for 30% solid concentration. The choice of velocity contours for exemplary suspension concentration allowed the observation of changes in the synthesis gas velocity rate along the column height. The maximal syngas velocity profile is located in the middle position of the bubble column. The average gas holdups also depend on the positions of the synthesis gas bubbles distributor. Fig. 5 presents gradient maps where black arrows indicate the gas flow direction. Pathlines colored by particles for 50 seconds time have been presented in Fig. 5 on the right. It allows setting a dead zone where the syngas does not flow. Pathlines of turbulent viscosity and velocity profile of bubble flowing are presented in Figs. 6 a-b). High solids concentration and lower syngas velocity would result in significant lowering of the turbulence regime in the column. In Fig. 6 c) we can see a pressure profile of the slurry bubble column. The pressure drop of the syngas flowing is proportional to the column height and also depends on syngas velocity on the inlet and slurry concentration. For

example, for the syngas inlet velocity 0.2 m/s and 10 % of the slurry concentration, the pressure drop is about 70 kPa.

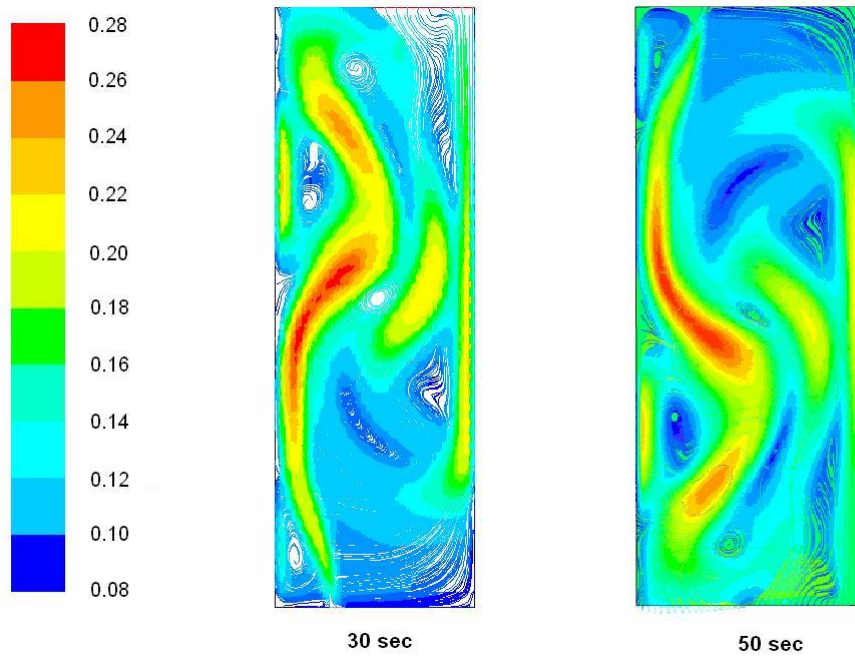


Fig. 4. Streamlines of syngas velocity profile for 30s and 50s (0.2 m/s velocity on inlet)

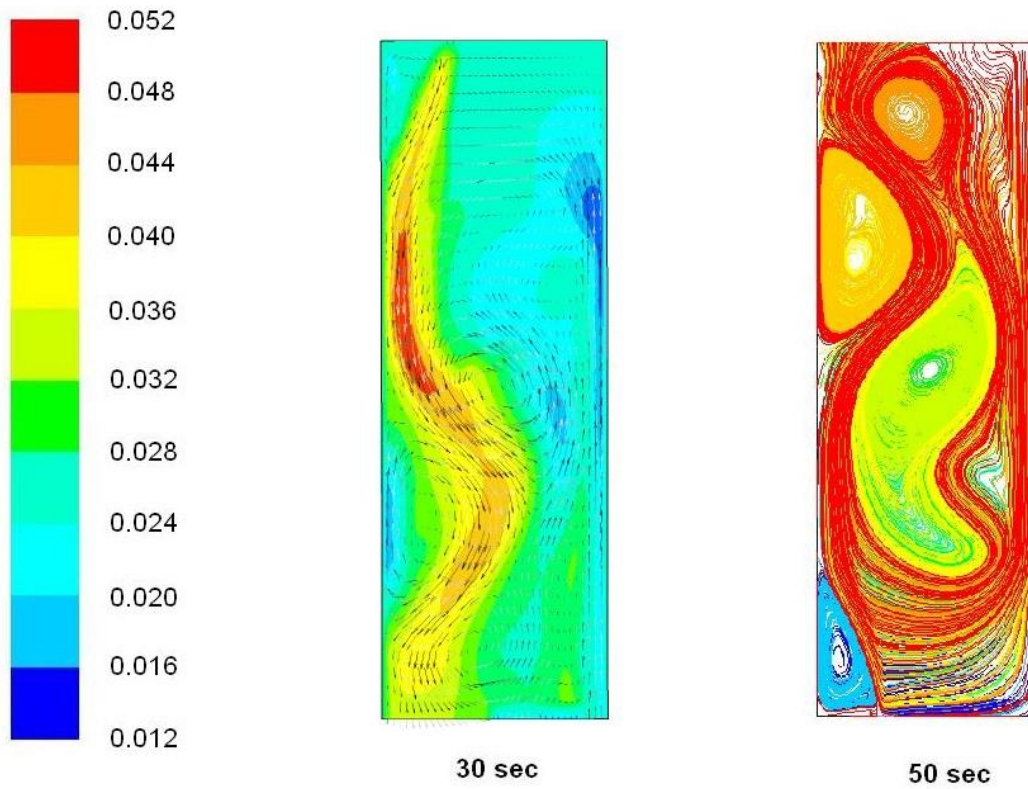


Fig. 5. Gradients map and pathline profile of the syngas flow for 30s and 50s (0.2 m/s velocity on inlet)

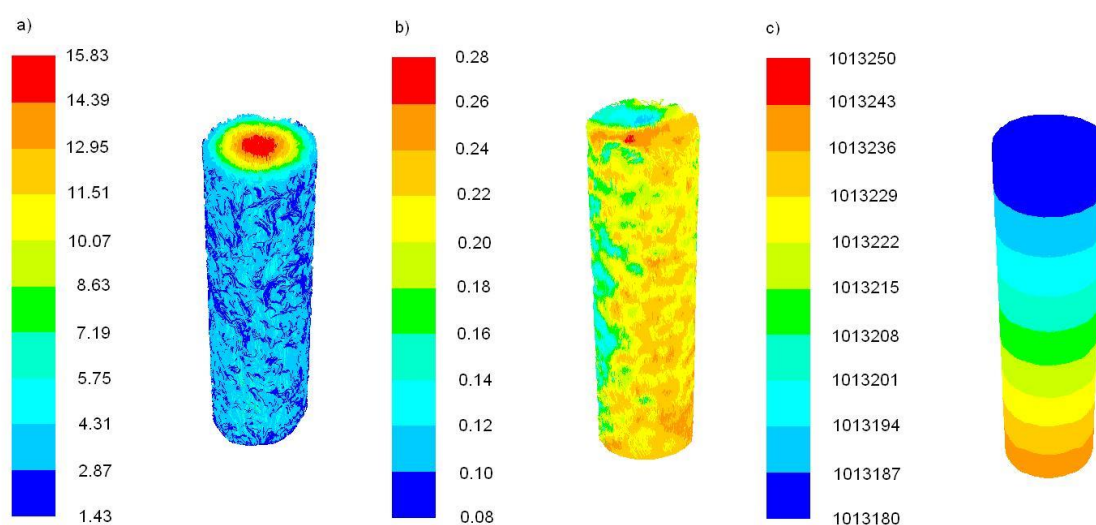


Fig. 6. 3D pathlines of eddy viscosity distribution a) syngas bubbles velocity b) sample pressure profile c) (0.2 m/s velocity on inlet)

In order to understand the effect of superficial velocity of the gas hold up, the simulation was carried out for different velocity inlets of the range 0.05 to 0.3 m/s and solid concentration (0-50 % vol). Fig. 7 presents the diagram of gas holdups for varying slurry concentrations and gas velocities. The gas holdup decreased due to the addition of solids which increased the concentration of the slurry phase. This can be due to bubbles break-up by the presence of larger amounts of suspended solids concentration. In turn, increasing velocity of the synthesis gas at the inlet decreased the gas hold-up. This was due to occurring events such as dynamic bubble break-up and coalescence. Bubble break-up was shown to increase at a faster rate by increasing the gas velocities compared to the bubble coalescence. Along with decreasing the velocity inlet, the residence time also decreased and caused reducing the total gas holdup in the bubble column.

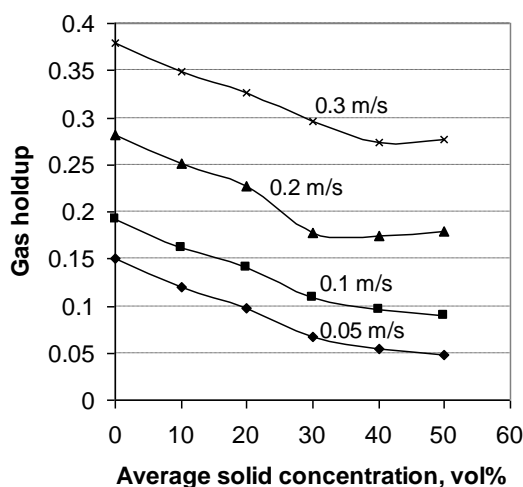


Fig. 7. Average bulk region gas holdups for varying slurry concentrations and gas velocities

Fig. 8 presents axial location of the gas holdup profiles for varying superficial gas velocities in syngas-slurry system. As shown above, by increasing the superficial gas velocity at the column inlet, a greater gradient degree of gas holdup along the column axis would be observed. The highest concentrations of the syngas bubbles which were present in the upper part of the column was caused due to a higher proportion of the bubbles breakup and the coalescence phenomenon.

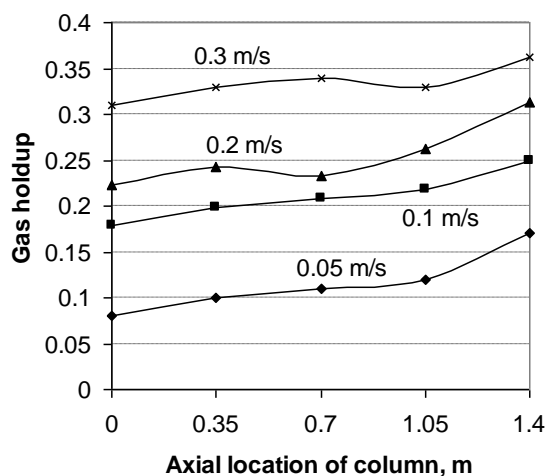


Fig. 8. Axial gas holdup profiles for varying superficial gas velocities along the column length

Fig. 9 presents average Sauter diameter for axial position along the column for different degrees of solid loading of the catalyst in slurry phase at syngas inlet velocity 0.2m/s. As shown, by increasing loading of the solid phase it also decreased the syngas bubbles diameter. The diameter of the synthesis gas diameter also changed along the column height. Some discrepancies including a change of the bubble diameter were caused by gas dilution and mechanical phenomena such as coalescence/breakup. Sauter diameter shapes were similar to the parabolic shape, which is also confirmed by the literature.

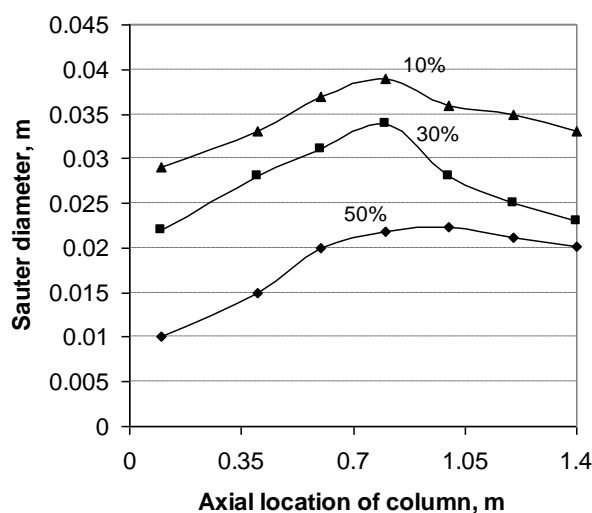


Fig. 9. Axial location of Sauter diameter along bubble column for different catalyst concentrations at syngas velocity inlet 0.3 m/s

All the simulations above were run in a Windows machine using a four parallel processing processors with 2.83 GHz performance. Computational cost which also increased quite for simulation lasted about 15 hours.

6. Conclusions

A CFD hydrodynamics model analysis of syngas flows through slurry bubble column was developed. Based on Ansys Fluent numerical simulation, the influence of inlet synthesis gas superficial velocity and suspension concentration gradients of the gas holdup were analyzed. Axial gas holdups enhanced by increasing the inlet syngas velocity and decreased by increasing the slurry concentrations in the column. In the case of slurry concentration, growth was attributed to the decrease in bubble breakup rate. The effect of gas velocity on the axial solids holdup profile was approximately parabolic.

Detailed prediction of such distribution can provide valuable practical information for catalyst concentration gradients location and improves the column design. Numerical calculations with predictions of syngas-slurry hydrodynamics behaviour provide valuable practical information such as gas holdup and solids concentration profiles. Methanol synthesis in slurry bubble column on heterogeneous catalyst can be a subject for further studies.

Nomenclature

Symbols

Y_q^j	mass fraction of species j in phase q
\vec{v}_q	velocity vector of phase q, m/s
D_q^j	diffusion coefficient of species j in phase q, kg/m/s
p	pressure, Pa
\vec{g}_q	gravity vector
K_{pq}	phase exchange coefficient between phases p and q, Ns/m ⁴
\vec{v}_q	velocity vector of phase q, m/s
ϵ	turbulent dissipation rate, m ² /s ³
k	turbulent kinetic energy, m ² /s ²
$\dot{m}_{gs,i}$	mass transfer rate between bubble classes due to interfacial mass transfer, kg/m ³ /s
d_i	bubble diameter, m
d_j	bubble smaller diameter, m
f_j	fraction of bubbles of class i
\bar{e}	average kinetic energy
S_{gj}	mass exchange rate due to coalesce and breakup, kg/m ³ /s
d_{32}	Sauter diameter
Re_{gs}	Reynolds number for gas-slurry phase
U_{gs}	superficial gas-solid velocity, m/s

σ_t turbulent Prandtl number binding kinematic viscosity solid phase

Greek symbols

α_q volume fraction of phase q

ε turbulent dissipation rate, m^2/s^3

ρ density, kg/m^3

σ_{sq} surface tension, N/m

τ stress tensor, Pa

λ eddy of size

μ_s dynamic coefficient of viscosity, $\text{kg}\cdot\text{m}^{-1}\cdot\text{s}^{-1}$

μ_{ts} kinematic viscosity of the liquid phase, $\text{m}^2\cdot\text{s}^{-1}$

Subscripts

g gas phase

m mixture

s slurry phase

l liquid phase

cat catalyst phase

References

- [1] B.Tabiś, R. Grzywacz, "Numerical and technological properties of bubble column bioreactors for aerobic processes". *Computers and Chemical Engineering* 35, 212-219, 2011 DOI: 10.1002/aic.690280302.
- [2] W.D Deckwer, E. Alper, "Katalytische Suspensions - Reaktoren", *Chem. Ing. Tech.* 52, 219–228, 1980.
- [3] P.Ramachandran, R. Chaudhari, "Three-phase Catalytic Reactors. Gordon and Breach" NewYork, NY. 1983.
- [4] Y.T.Shah, S.Joseph, D.N.Smith, J.A.Ruether, "Two-bubble class model for churn turbulent bubble-column reactor". *Ind. Eng.Chem.Process Des. Dev.* 24, 1985, 1096–1104.
- [5] N.Rados, M.H. Al-Dahhan, M.P Dudukovic, "Dynamic modeling of slurry bubble column reactors". *Ind.Eng.Chem.Res.* 44, 6086–6094, 2005.
- [6] M.Henze M., G. Leslie, C. P.,Gujer, W.Marais, T. Matsuo, "A general model for single-sludge wastewater treatment systems." *Water Research*, 21, 405–515, 1987.
- [7] R.Krishna, J. Swart, J. Ellenberger, G.B. Martina, C.Maretto, "Gas holdup in slurry bubble columns: effect of column diameter and slurry concentrations". *AIChEJ* 43, 311–316, 1996.
- [8] K.Ekambara, J.B. Joshi, "CFD simulation of mixing and dispersion in bubble columns." *Chem. Eng. Res. Des.* 81, 987–1002, 2003.
- [9] S.Schluter, A.Steiff, P.M. Weinspach, "Modelling and simulation of bubble column reactors." *Chem.Eng.Process.* 31, 97–117, 1992.
- [10] A.Troshko, F. Zdravistch, "CFD modeling of slurry bubble column reactors for Fisher–Tropsch synthesis", *Chemical Engineering Science* 64 (2009) 892 – 903.

- [11] P.Chen, J. Sanyal, M.P.Dudukovic, "Numerical simulation of bubble columns flows: effect of different breakup and coalescence closures." *Chemical Engineering Science* 60, 1085–1101, 2005.
- [12] R.Krishna, J.Ellenberger, "Gas hold up in bubble column reactors operating in the churn-turbulent flow regime". *AIChEJ* 42, 2627–2634,1997.
- [13] Q.Nana, K.Zhang, Y. Yong, "CFD Simulation of Hydrodynamics in Bubble Columns with Perforated Plate Distributor." *International Conference Materials for Renewable Energy and Environment (ICMREE)* 3, 703-707,2013.DOI: 10.1109/ICMREE.2013.6893774
- [14] P.Klug, A.Vogelpohl A, " Bubble formation at sieve plates-effects on gas hold up in bubble columns." *Ger. Chem. Engng* 9, 93-101,1986.
- [15] P.Chen, M.P. Dudukovic, J. Sanyal, "Three-dimensional simulation of bubble column flows with bubble coalescence and breakup." *Fluid Mechanics and Transport Phenomena* 51 (3), 696–712, 2005.
- [16] P.Mills, "The Fischer–Tropsch synthesis in slurry bubble column reactors: analysis of reactor performance using the axial dispersion model". *Fuel Energy* 77,1997.
- [17] S.Saxena," Bubble column reactors and Fischer–Tropsch synthesis. *Catalysis Reviews—Science and Engineering* 37 (2), 227–309,1995."
- [18] A.Wodołażski, P.Mocek, I.Gil, E.Jędrysik, "Gas dynamics of stack-type microreactors with various filling shape." *Przem. Chem.* 92, 3, 374,2013.
- [19] A.Wodołażski, "Modeling of the methanol synthesis in plate microreactor. *Electrical Review.* 1, 76, 2014. DOI:10.12915/pe..01.18.
- [20] J.Hinze," Turbulence," McGraw-Hill Book Co., NY, 1975
- [21] M.Ishii and N.Zuber," Drag coefficient and relative velocity in bubbly, droplet or particulate flows" *A/ChE J.*, 1979, vol. 25, pp. 843-55.
- [22] A.Cockx, Z. Do-Quang, M. Roustan, "Use of computational fluid dynamics for simulating hydrodynamics and mass transfer in industrial ozonation towers." *Chem. Engng Sci.* 54, 5085–5090,1999.
- [23] Weibin S., Yang N., Yang X., "A kinetic inlet model for CFD simulation of large-scale bubble columns *Chemical Engineering Science* 158 (2017) 108 – 116, 2017.
- [24] A. Wodołażski , "Modelling of slurry hydrodynamics with two-blade impeller in tank reactor ". *Maintenance and Reliability.* 16 (4), 533–536, 2014.
- [25] N. Rados, M.H. Al-Dahhan, M.P. Dudukovic. "Modeling of the Fischer–Tropsch synthesis in slurry bubble column reactors." *Catal. Today* 79, 211–218, 2003.

آنالیز CFD هیدرودینامیک جریان گاز سنتز در ستون حبابی دوغاب

آرتور ودولاژسکی^{۱*}

^۱ انستیتو مرکزی معدن، لهستان

چکیده

در مقاله حاضر، مدل‌سازی CFD جریان گاز سنتز در ستون حبابی دوغاب توسعه داده شده است. این مدل بر اساس دیدگاه اولری-اولری است و سه فاز را در بر می‌گیرد: دوغاب ذره‌های جامد معلق در روغن پرافین و حباب گازهای سنتزی. محاسبات عددی انجام شده جهت ذره‌های کاتالیزور، انعقاد و شکست حباب شامل نیروی کشش حباب-مایع و اثرات سطوح فصل مشترک را شامل می‌شد. همچنین اثرات ذره‌های جامد موجود در فاز مایع توصیف گردیدند.

مشخصات مقاله

تاریخچه مقاله:

دریافت: ۹ اردیبهشت ۱۳۹۵

پذیرش نهایی: ۱ آذر ۱۳۹۵

کلمات کلیدی:

هیدرودینامیک

ستون حبابی دوغاب

مدلسازی CFD

* عهده‌دار مکاتبات؛

رایانامه:

awodolazski@gig.katowice.pl

تلفن: +۴۸ ۳۲ ۳۲۴۶۵۲۸

دورنگار: +۴۸ ۳۲ ۳۲۴۶۵۲۸